

DYNAMIC BEHAVIOUR OF A STRENGTHENED POINTED ARCH TESTED ON SHAKING TABLE

Paulo Šćulac¹, Nina Čeh¹, and Matei Cukarić²

¹ University of Rijeka, Faculty of Civil Engineering
Radmile Matejčić 3, 51000 Rijeka
e-mail: {paulo.sculac,nina.ceh}@uniri.hr

² Koning Projekt d.o.o
Spinčičeva 4, 52100 Pula
matei.cukaric@gmail.com

Abstract

This paper presents an experimental study of a strengthened pointed arch subjected to horizontal sinusoidal excitation on a shaking table. The geometry of the arch was selected to represent the geometry of typical Gothic vaults found in small single-nave village churches in Istria with preserved medieval wall paintings. The arch model was constructed from identical timber blocks with dry joints, while the reinforcement (duct tape) was applied either at extrados or at intrados of the arch. The aim of this study was to document the dynamic behaviour of pointed arches strengthened with composites, since there is a lack of experimental tests on this type of geometry. Contactless optical measuring system was used to monitor the openings between the blocks, since conventional sensors are difficult to apply. Two high-speed cameras made it possible to record the formation and closure of hinges between the blocks. Due to strengthening some hinges were hindered and consequently the seismic capacity of the arch was significantly improved.

Keywords: Masonry, Pointed Arch, Strengthening of Arches, DIC, Shaking Table Test, Collapse Mechanisms.

1 INTRODUCTION

Strengthening of existing masonry buildings is a topic that is increasingly being researched in order to extend the design life of structures and preserve historic buildings. At present, researches are mostly dealing with methods that use steel, carbon or glass fibers in fiber-reinforced polymers (FRP) and textile-reinforced mortar (TRM) systems, as well as steel ties or other fibrous materials that could be used as reinforcing materials for masonry arches and vaults [1, 2, 3, 4, 5]. According to the principles from ISCARSAH recommendations for the structural restoration of protected architectural heritage special attention must be given to the selection of the appropriate retrofitting method in order to satisfy compatibility with existing materials, reversibility and lowest impact criteria (keeping interventions to the minimum to guarantee safety and durability) [6]. This especially applies to strengthening methods regarding new composite materials.

The behaviour of arches is usually analyzed on a four-link model with three rigid blocks (consisting of multiple masonry stone or brick blocks) interconnected by four hinges occurring alternately at the extrados and at intrados of the arch [7]. The collapse of an arch depends on its geometry rather than on its material properties (masonry strength), i.e. the collapse will occur due to loss of stability without material failure.

In case of composite reinforcement applied at extrados or/and at intrados of the arch the failure mode is changed significantly: due to reinforcement the formation of the fourth hinge will usually be prevented. This means that the collapse will not occur due to transformation of the arch into a mechanism but due to other failure mechanisms related to reinforcement, such as composite rupture and composite detachment (bond failure), shear sliding of blocks or due to masonry crushing [1, 4].

Pointed arches and vaults give smaller values of thrust than circular arches and can be made thinner than circular arches for large angles of embrace [8]. Although they are quite widespread (they are essential both in the Islamic architecture and in the architecture from the Gothic period) there is still a lack of numerical and experimental studies of strengthening on this type of geometry.

To date, only few shaking table tests have been conducted on strengthened arches and vaults (only with circular geometry). Castellano et al. [9] performed dynamic tests on a full-scale tuff masonry semi-circular arch strengthened at extrados with a 5 mm thick glass fabric reinforced cementitious matrix. As expected, the reinforcement prevented the opening of hinges at the intrados and a substantial increase of the seismic capacity of the arch. Giamundo et al. [10] conducted shaking table tests of a full-scale clay brick masonry segmental barrel vault. Tests have been first performed on the unreinforced vault; the vault was then strengthened with inorganic matrix applied at the extrados of the vault and tested again to investigate the effects of the retrofitting.

Tilting tests are often used as a static approximation of the shaking table tests (see e.g. [11, 12]). In this simplified alternative, the base with the scaled model is gradually tilted up until the collapse of the model. The tangent of the angle at which the collapse occurs corresponds to the base acceleration at which the model is transformed into a mechanism. In case of arch with dry joints strengthened at extrados or at intrados, it is not possible to use the tilt tests to obtain the base acceleration. Instead of one hinge, the crack opening is smeared over a greater area (i.e. several narrow hinges will open in adjacent blocks interconnected by reinforcement) and unrealistic large results are obtained.

This paper summarizes some preliminary results of a pointed arch model with dry joints tested on shaking table. Arch was strengthened either at extrados or at intrados and subjected to sinusoidal base excitation with fixed amplitude and increasing frequency.

2 EXPERIMENTAL SETUP

The geometry of the arch was selected to represent the geometry of pointed barrel vaults found in more than 15 small single-nave Gothic churches in Istria with preserved medieval wall paintings, which are protected as cultural heritage (Figure 1). Churches with wall paintings are an essential part of the Istrian cultural identity; so far, more than 140 sites with fresco paintings dating from the 8th to the 17th century have been investigated and documented [13].



Figure 1: Single-nave churches with pointed vaults in Istria.

A rather simple experimental model has been designed, due to the fact that the collapse of an arch depends on its geometry rather than on material strength. The model was made of timber blocks – beech was chosen because it has sufficient strength in order to perform multiple tests without damaging the blocks. The arch was composed of 23 blocks: 22 blocks had the same trapezoidal form, while the keystone was cut in a triangular form and glued to the neighboring trapezoidal blocks thus making a three-block unit (Figure 2). In order to make the friction coefficient closer to dry-joint stone arches a sandpaper with grit size P150 was glued on the upper surface of each block. The total mass of the arch model was equal to 5207 g (mean mass value of a unit block was 207 g, while the three-block keystone had 653 g). Thickness orthogonally to the plane of the arch was 8 cm.

To allow rotation at the base and formation of hinges L-shaped aluminum profiles were used as supports, fastened to the timber base plank with open side placed downwards. The timber base was attached to the shaking platform *Quanser ST-III* (Figure 3).

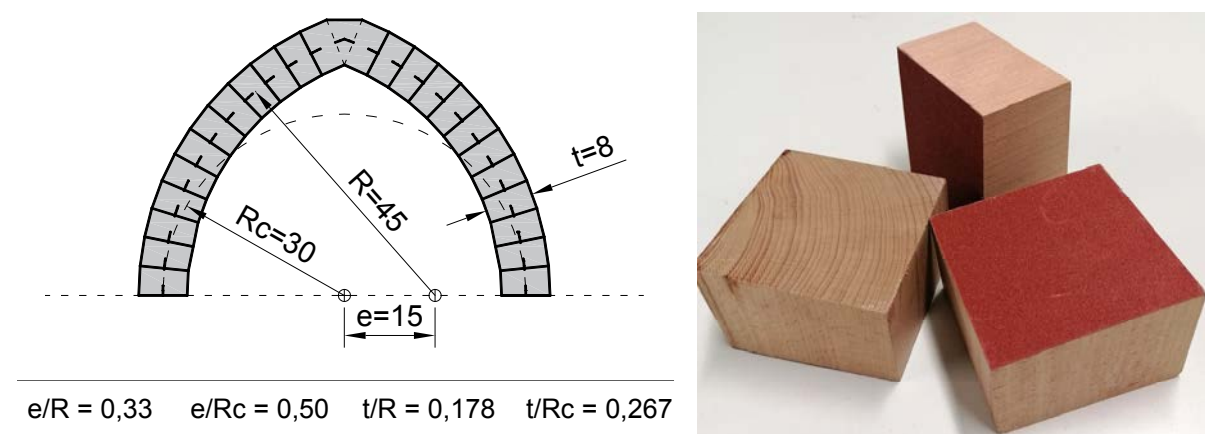


Figure 2: Geometry of the pointed arch (dimensions in cm) and timber blocks.

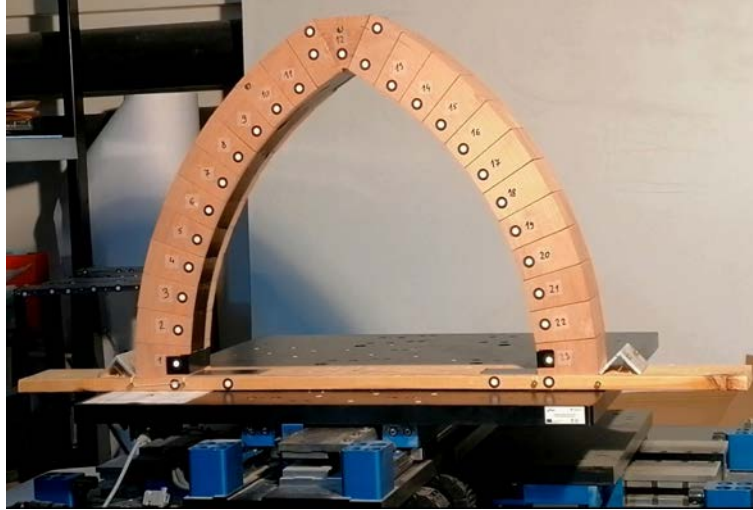


Figure 3: Experimental setup: arch model on the shaking platform.

Duct tape (*TEXO American Duct Tape*) was used as reinforcement, thereby trying to simulate the FRP or TRM strengthening system. One layer of tape, 50 mm wide and 0.19 mm thick, was applied either at extrados or at intrados of the arch. Mechanical properties of the tape were: tensile strength 31.6 N/cm, adhesion to steel 4.8 N/cm. The tape was made of PVC, PE and a fabric layer. Detail of tape anchorage to timber base is presented in Figure 4.

The model was monitored with a system for contactless optical measurement of 3D displacements and strains *GOM Aramis 4M* using a digital image correlation approach (DIC), which consisted of two high-speed cameras with a resolution of 2400×1728 pixels. Round point markers were attached to the front side of each block in order to detect any displacement change occurring at the contacts between the blocks. The experiment was tracked with 100 frames per second.

The base displacement of the platform was defined as a sinusoidal function:

$$d_{\text{base}}(t) = d_0 \cdot \sin(\omega t) \quad (1)$$

and the base acceleration was:

$$a_{\text{base}}(t) = -d_0 \cdot \omega^2 \cdot \sin(\omega t) \quad (2)$$

where d_0 is the maximum displacement of the base, ω is the natural frequency related to shaking table's frequency ($f = \omega/2\pi$) while t is time. The displacement amplitude of 2.5 cm was kept constant, while the frequency was increased starting from 0.25 Hz with steps of 0.25 Hz, and held piecewise constant throughout the experiment.

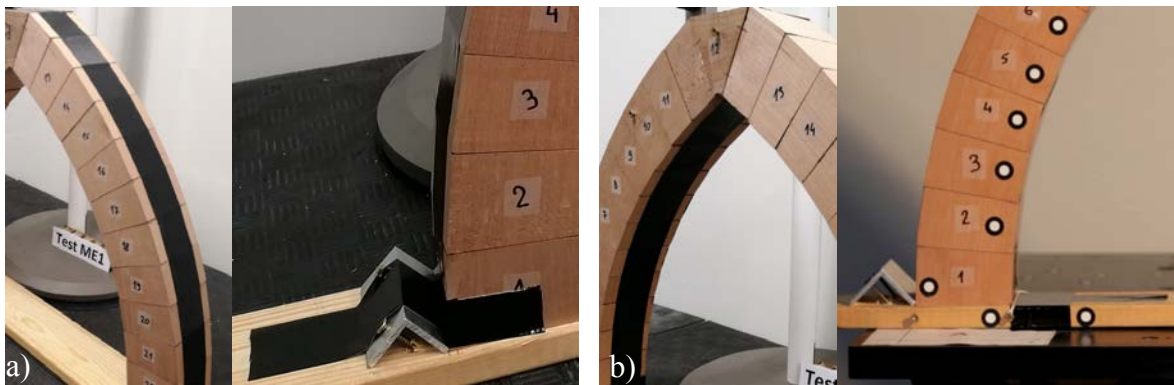


Figure 4: Reinforcement applied a) at extrados or b) at intrados of the arch and detail of anchorage.

3 RESULTS AND DISCUSSION

3.1 Un-strengthened arch

First, the results for the un-strengthened arch are presented. Figure 5 displays the base displacement and base acceleration time-history graphs. The peak acceleration in the final part of the experiment was 3.0 m/s^2 .

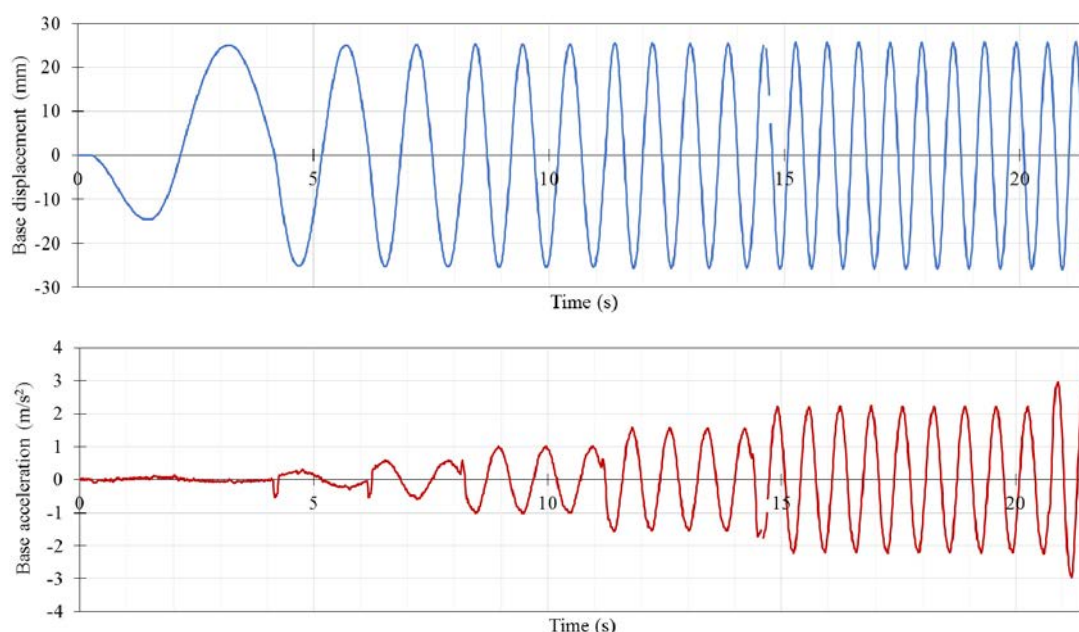


Figure 5: Base displacement and base acceleration time-history for un-strengthened arch ($f_{\max} = 1.75 \text{ Hz}$).

High speed cameras made it possible to record the formation of hinges and failure of the arch (Figure 7). Arch initially behaved as a rigid body, and there were no hinges visible to the naked eye until $t = 15 \text{ s}$. At about $t = 20 \text{ s}$ four hinges formed alternately at extrados and intrados of the arch. Due to base platform movement in the reverse direction, these hinges then closed but were soon followed by formation of four hinges in an alternate position (i.e. almost mirror symmetric). Note that the location of the hinges is not fixed during the base movement – closure of initial hinges followed by relocation may be observed. A more detailed discussion on the behaviour of a pointed arch tested on a shaking table is given in [14].

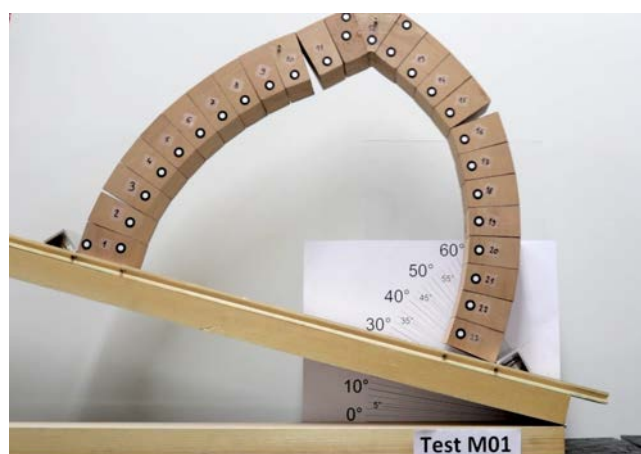


Figure 6: Tilting test (un-strengthened arch)

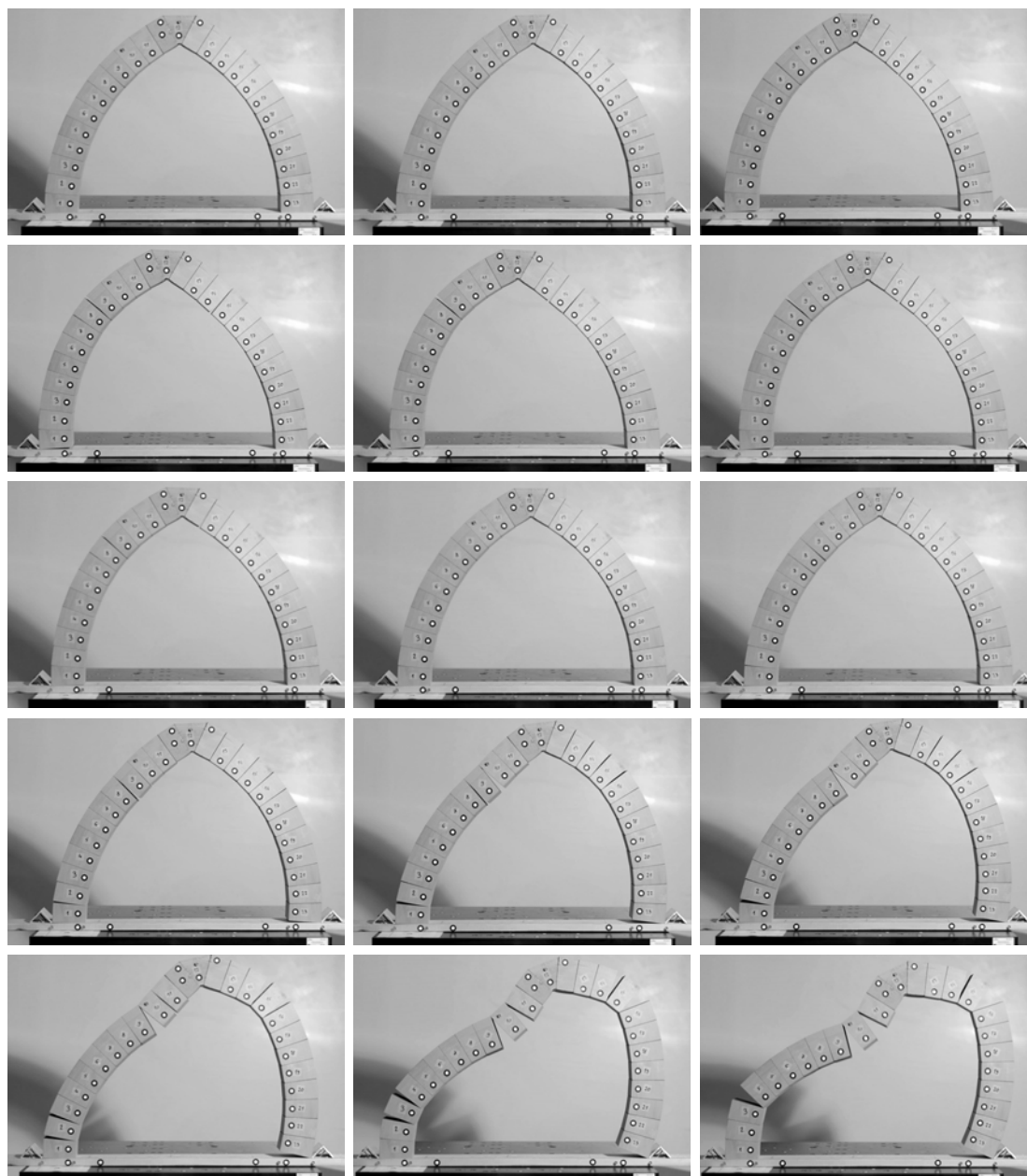


Figure 7: Series of photos documenting hinge formation in un-strengthened pointed arch.

Tilting tests were also conducted (Figure 6). Angle at which the arch transformed into a mechanism was between 16° and 18° , what corresponds to base acceleration $0.29g$ to $0.32g$, and is in good correlation with the maximum acceleration obtained on the shaking table test.

3.2 Arch strengthened at extrados

Figure 8 presents the base displacement and base acceleration time-history graphs for arch strengthened at extrados. Part of data that is missing on the graph is due to low quality of images (DIC wasn't able to provide data). The maximum base acceleration recorded was 4.9 m/s^2 – a notable increase with respect to the unreinforced arch. Note that the number of cycles that the arch could withstand prior to failure also increased.

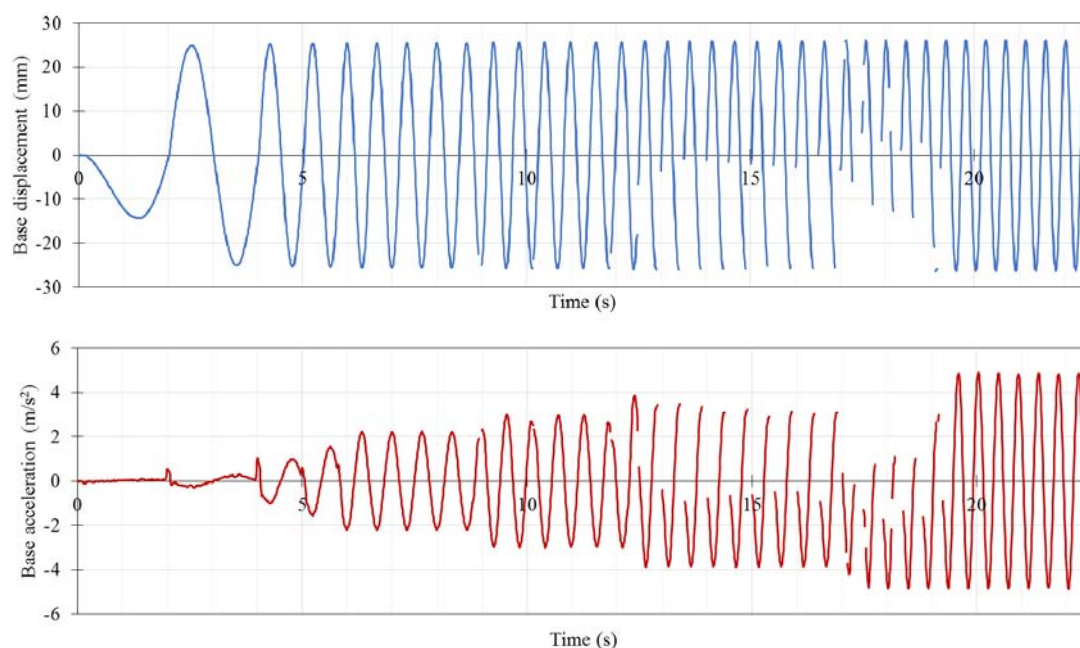


Figure 8: Base displacement and base acceleration time-history for arch strengthened at extrados ($f_{\max} = 2.25$ Hz).

The opening of some hinges is presented in Figure 9, where data series numbers denote the block numbers (for block numeration see Figure 3), while “B” is the base (for example “distance 6-7” denotes the distance between the round point markers located on blocks 6 and 7). Opening and closing of hinges follow the sinusoidal movement of the shaking table.

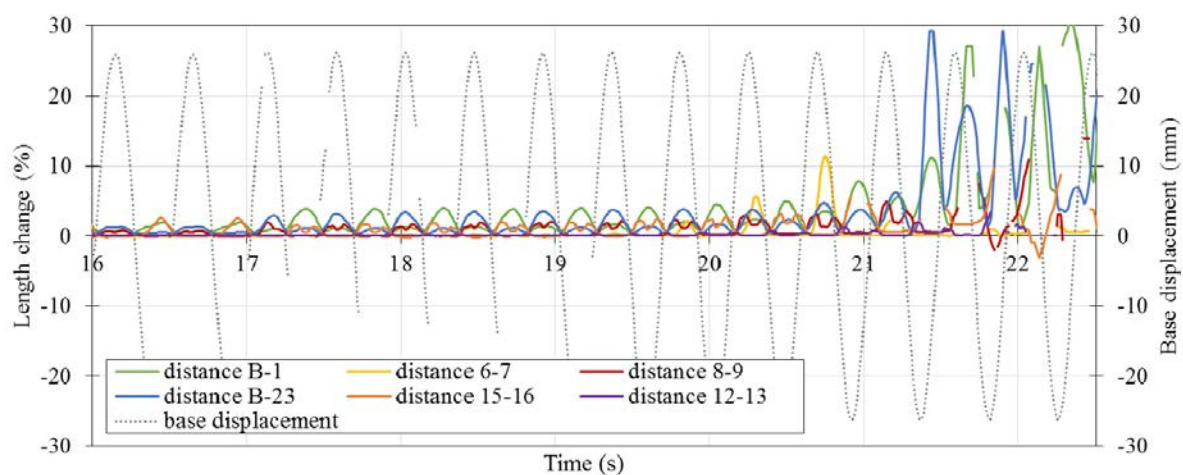


Figure 9: Tracking of openings between blocks via DIC (arch strengthened at extrados).

Figure 10 reports the shaking table testing of arch strengthened at extrados. The failure mechanism differs from the model without reinforcement - the reinforcement applied at extrados prevented opening of hinges at intrados and caused rocking. Finally, the failure occurred due to loss of anchorage at supports, debonding of the tape and shear sliding. The tensile strength of the reinforcement was actually improperly too high selected so that no rupture occurred.



Figure 10: Series of photos documenting testing of pointed arch strengthened at extrados.

3.3 Arch strengthened at intrados

Figure 11 presents the base displacement and base acceleration time-history graphs for arch strengthened at intrados. Again, the reinforcement prevented opening of hinges - in this case at the extrados, since the reinforcement is applied at intrados.

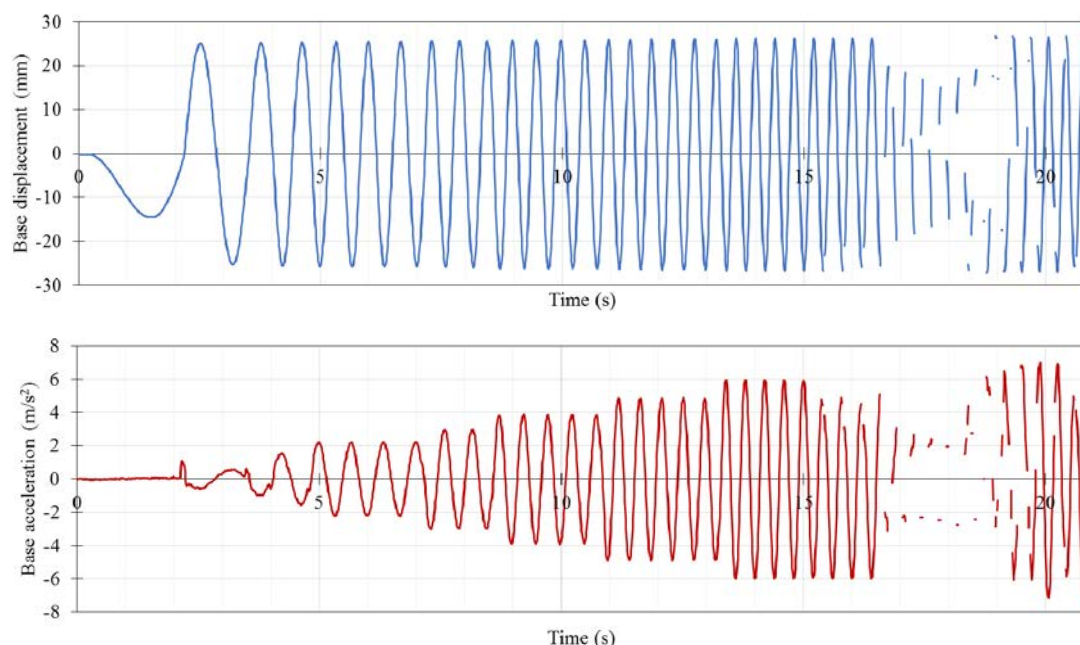


Figure 11: Base displacement and base acceleration time-history for arch strengthened at intrados ($f_{\max} = 2.75$ Hz).

The maximum base acceleration recorded was 7.15 m/s^2 , which is a significant increase when compared with un-strengthened arch, but also with arch strengthened at extrados. This can be attributed to better anchorage of the duct tape to the base plank – in case of intrados strengthening an additional string has been added at the model-base plank joint to hold the tape tightly connected to the base. In the end, it was this string that actually caused the tape to break (the string cut the tape).

Tracking of some hinges is presented in Figure 12, while Figure 13 documents the failure of the arch.

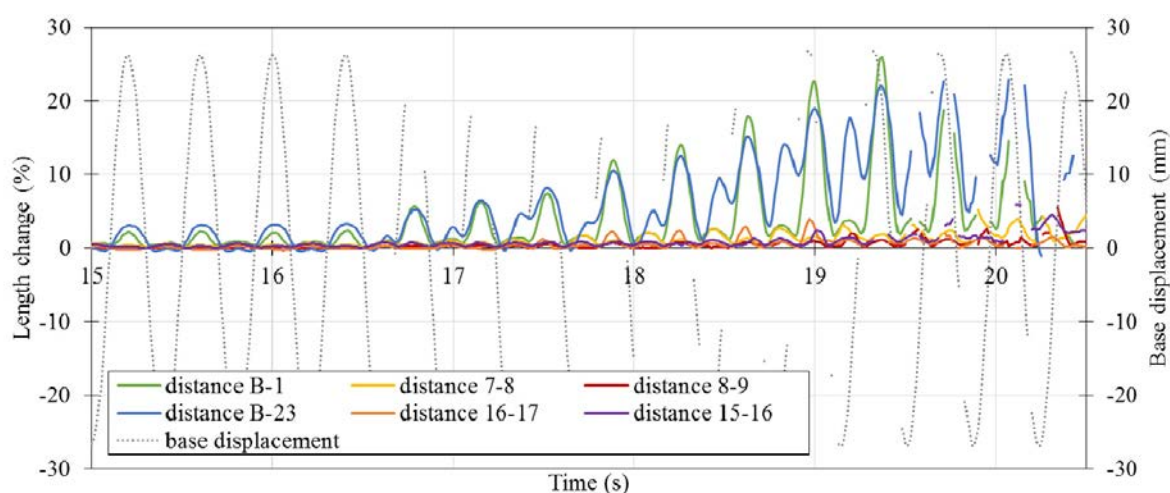


Figure 12: Tracking of openings between blocks via DIC (arch strengthened at intrados).

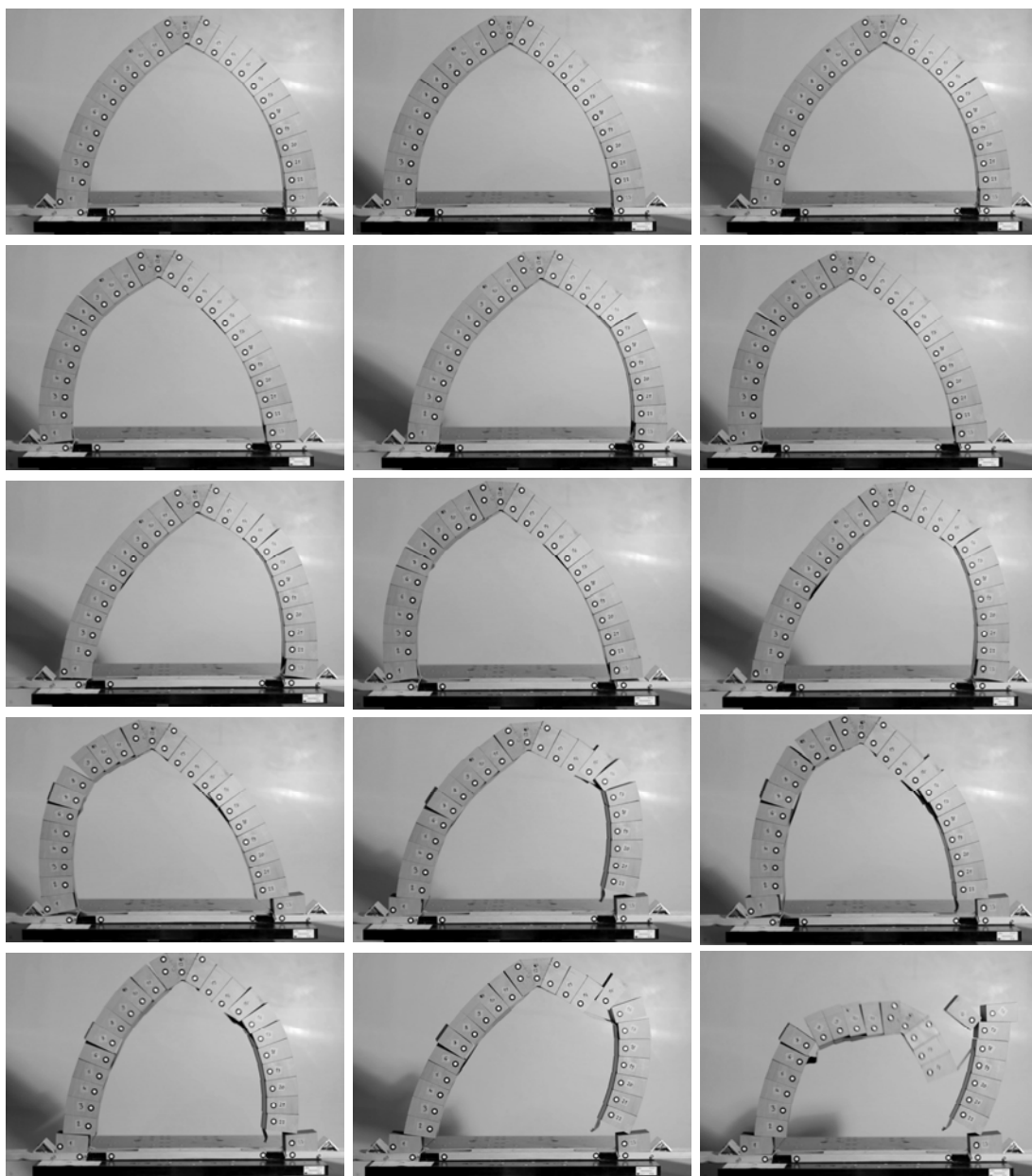


Figure 13: Series of photos documenting testing of pointed arch strengthened at intrados.

4 CONCLUSIONS

- In this paper we presented pre-collapse dynamic behaviour of a strengthened pointed arch. To date, shaking table tests haven't been conducted on strengthened pointed arches.
- The arch model was constructed from identical timber blocks with dry joints and subjected to a sinusoidal excitation. Duct tape was used as the strengthening material, simulating FRP/TRM reinforcement, applied either at extrados or intrados of the arch. Although the model is rather simple and low-cost, it can still provide valuable results.
- Due to effect of reinforcement some hinges were hindered, and the seismic capacity was significantly increased for both reinforcing types. The collapse was due to debonding and shear sliding. Arch reinforced at intrados was able to withstand greater base acceleration what is attributed to better anchorage of the reinforcing tape to the base plank.

5 ACKNOWLEDGEMENTS

The Authors thank the University of Rijeka for supporting the publication of this paper through grants ZIP-UNIRI-1500-3-20, uniri-mladi-tehnic-20-41 2645 and uniri-tehnic-18-127.

REFERENCES

- [1] P. Zampieri, N. Simoncelo, C.D. Tetougueni, C. Pellegrino, A review of methods for strengthening of masonry arches with composite materials. *Engineering Structures*, **171**, 154-169, 2018.
- [2] G. Misseri, L. Rovero, G. Stipo, S. Barducci, V. Alecci, M. De Stefano, Experimental and analytical investigations on sustainable and innovative strengthening systems for masonry arches. *Composite Structures*, **210**, 526-537, 2019.
- [3] F.G. Carozzi, C. Poggi, E. Bertolesi, G. Milani, Ancient masonry arches and vaults strengthened with TRM, SRG and FRP composites: Experimental evaluation. *Composite Structures*, **187**, 466-480, 2017.
- [4] A. Borri, P. Casadei, G. Castori, J. Hammond, Strengthening of brick masonry arches with externally bonded steel reinforced composites. *Journal of Composites for Construction (ASCE)*, **13**, 468-475, 2009.
- [5] C. Chisari, D. Cacace, G. De Matteis, Parametric Investigation on the Effectiveness of FRM-Retrofitting in Masonry Buttressed Arches. *Buildings*, **11**, 406, 2021.
- [6] P. Roca, P.B. Lourenço, A. Gaetani, *Historic Construction and Conservation: Materials, Systems and Damage*. Routledge, 2019.
- [7] F. Di Carlo, S. Coccia, M. Piedigrossi, Dynamics of masonry pointed arches under base motion. *International Journal of Masonry Research and Innovation*. **2**(4), 335-354, 2017.
- [8] A. Romano, J.A. Ochsendorf, The mechanics of gothic masonry arches. *International Journal of Architectural Heritage*, **4**(1), 59-82, 2010.
- [9] A. Castellano, A. Fraddosio, J. Scacco, G. Milani, M.D. Piccioni, Dynamic Response of FRCM Reinforced Masonry Arches. *Key Engineering Materials*, **817**, 285-292, 2019.
- [10] V. Giamundo, G.P. Lignola, G. Maddaloni, F. da Porto, A. Prota, G. Manfredi, Shaking table tests on a full-scale unreinforced and IMG-retrofitted clay brick masonry barrel vault. *Bulletin of Earthquake Engineering*, **14**, 1663–1693, 2016.
- [11] G. Misseri, M.J. DeJong, L. Rovero, Experimental and numerical investigation of the collapse of pointed masonry arches under quasi-static horizontal loading. *Engineering Structures*, **173**, 180-190, 2018.
- [12] A. Gaetani, P.B. Lourenço, G. Monti, M. Moroni, Shaking table tests and numerical analyses on a scaled dry-joint arch undergoing windowed sine pulses. *Bulletin of Earthquake Engineering*, **15**, 4939-4961, 2017.
- [13] Ž. Bistrović, *Colourful trail of Istrian frescoes*. Istria County, Pula, 2011.
- [14] P. Šćulac, N. Čeh, Experimental test on a pointed arch model monitored by contactless optical system. *International Journal of Masonry Research and Innovation*, 1-16, 2023.